Available online at www.sciencedirect.com
ScienceDirect
Physica C 468 (2008) 60–65
PHYSICA C
www.elsevier.com/locate/physc

The normal state transport properties of $NdBa_{2-x}La_xCu_3O_{7-\delta}$: Evidence of localization hole by La

S.R. Ghorbani *, E. Rostamabadi

Department of Physics, Tarbiat Moallem University of Sabzevar, Sabzevar, Iran

Received 19 June 2007; accepted 23 October 2007
Available online 30 October 2007

Abstract

The transport properties of sintered samples $NdBa_{2-x}La_xCu_3O_{7-\delta}$ with $0 \leqslant x \leqslant 0.30$ have been studied in the normal state by X-ray diffraction, the resistivity, and the thermoelectric power measurements. La doping results in a larger normal state resistivity, the thermoelectric power, a lower critical temperature T_c, a larger pseoudogap temperature T_g, and a change from a metal-like to a semiconductor-like behavior at low temperature and high doping concentration. The strong increase in the room temperature resistivity for $x \geqslant 0.05$ suggested that hole filling picture is not only mechanism to decrease hole concentration but there is also another mechanism such as mobile hole localization. The results of the resistivity as a function of temperature and doping concentration was analyzed within bipolaron model while the thermoelectric power was analyzed within a phenomenological narrow band model. A good agreement between models and data were obtained. An increased tendency for localization is found within both models. Therefore, the results of both models suggested that both hole localization and hole filling mechanisms decrease the hole concentration.
© 2007 Elsevier B.V. All rights reserved.

PACS: 74.72.−h; 74.72.Jt; 74.62.Dh

Keywords: Transport properties; $NdBa_{2-x}La_xCu_3O_{7-\delta}$; Hole localization

1. Introduction

In high-temperature superconductors the strong sensitivity of the superconducting critical temperature T_c to dopants has been a challenging problem from the discovery of superconductivity. Experiments on the normal state transport properties such as the resistivity and the thermoelectric power have revealed a close relationship between the electronic properties of the oxide superconductor and the hole carrier concentration within the CuO_2 planes [1]. Therefore, they are important for understanding the mechanism of oxide superconductivity.

The thermoelectric power is highly sensitive to the details of the charge concentration. In polycrystalline samples, grain boundaries will have less effect on the thermoelectric power than on the electrical conductivity because the temperature drop between grains will usually be insignificant while the voltage drop is not.

Some common features of the transport properties have been found in high-T_c superconductors, HTS, such as the relation between hole concentration in CuO_2 plane and the room temperature thermoelectric power [2] and the critical temperature [3,4]. There is still no satisfactory explanation for the behavior of transport properties such as the thermoelectric power and the in-plane resistivity and wealth of theoretical models and experiments remain controversial. Several models have been proposed to describe the resistivity and the thermoelectric power such as Andersson's Luttinger-liquid model [5], (bi)polaron model [6], and a phenomenological narrow band model [7].

In the present paper we have made systematic studies of the effect of La on the Ba site into the $NdBa_2Cu_3O_{7-\delta}$ system by the X-ray diffraction, the resistivity, and the

* Corresponding author. Fax: +98 5714411161.
E-mail address: ghorbani@sttu.ac.ir (S.R. Ghorbani).

0921-4534/$ - see front matter © 2007 Elsevier B.V. All rights reserved.
doi:10.1016/j.physc.2007.10.013

thermoelectric power measurements. From the room temperature thermoelectric power the hole concentration was estimated. The hole concentration changed with La doping, which was consistent with the change in the resistivity, the thermoelectric power, and the superconducting critical temperature. The normal state transport properties were analyzed and well described by a phenomenological narrow band and the bipolaron models. These models description suggest that both hole filling and mobile hole localization are the reason for the observed strong increase of the in-plane resistivity and suppression superconductivity.

2. Experimental details

Polycrystalline samples of $NdBa_{2-x}La_xCu_3O_{7-\delta}$ with $x = 0$, 0.05, 0.10, 0.15, 0.20, and 0.30 were prepared by standard solid-state methods. Starting materials were high purity Nd_2O_3, $BaCO_3$, CuO, and La_2O_3. The samples were pressed into pellets and calcinated at 900, 920, and 920 °C in air with intermediate grindings. They were then annealed in flowing oxygen at 460 °C for 3 days and the temperature was finally decreased to room temperature at a rate of 12 °C/h.

The samples were characterized by X-ray powder diffraction (XRD). The XRD patterns were recorded in a Guinier-Hägg focusing camera using Cu Kα radiation with Si as an internal standard, and the photographs were evaluated in a micro-densitometer system [8]. This is a sensitive technique for detection of impurity phases with an estimated sensitivity level of a few percent of crystalline impurities. The XRD results for La-doped Nd-123 samples displayed a single-phase orthorhombic structure at all doping levels.

The electrical resistivity was measured with a standard dc four-probe method. Electrical leads were attached to the samples by silver paint and heat treated at 300 °C in flowing oxygen for half an hour, which gave contact resistances of order 1–2 Ω. Thermoelectric power measurements were made on sintered bars of typical dimensions $0.5 \times 2.5 \times 8$ mm^3, using a small, and reversible temperature difference of 2 K. The data were corrected for the contribution of the copper connecting leads.

3. Results and analyses

The samples were characterized by XRD. The XRD results for all samples displayed single-phase orthorhombic space group (*Pmmm*) structure. The effects of La substitution on the lattice constants are shown in Fig. 1. The increase of smaller La atom results in a compression of the unit cell (Fig. 1b) with an approximately linear decrease in the *c*, an increase in the *a,* and a decrease in the *b*-axis length. The increase of the *a*-axis and the decrease of the *b*-axis cause the orthorhombicity to decrease. This is accompanied by an increase in the O5 occupancy, pointing at an increased disorder in the Cu–O chains with increasing La doping concentration.

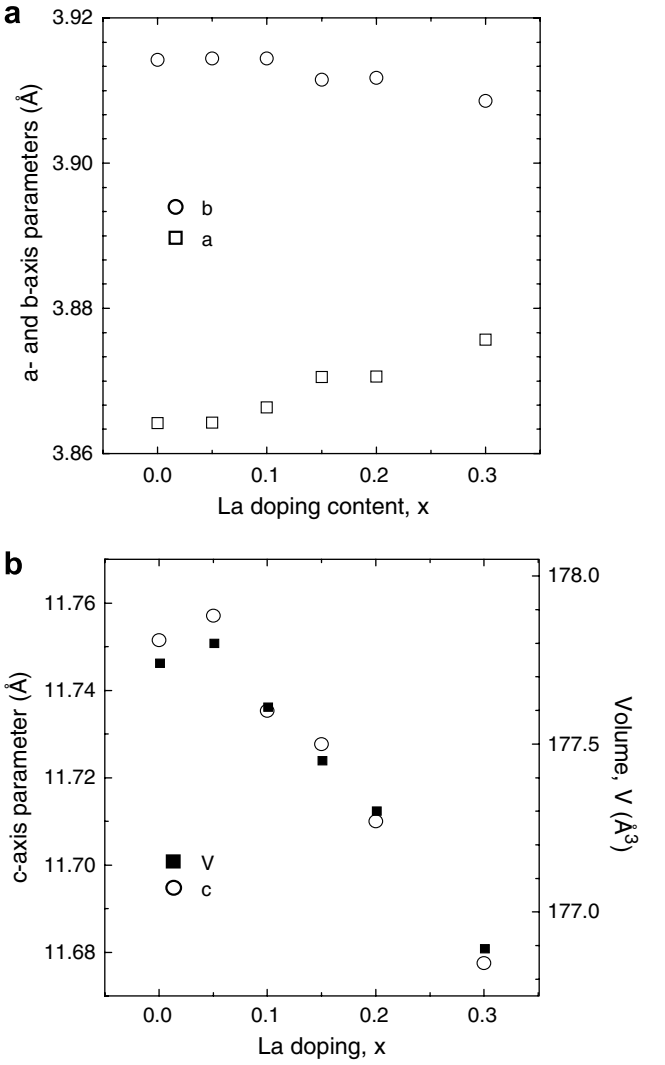

Fig. 1. (a) *a*- and *b*-axis lattice parameters, (b) *c*-axis lattice parameter and the cell volume versus doping concentration for $NdBa_{2-x}La_xCu_3O_{7-\delta}$.

The temperature dependence of the thermoelectric power *S* is shown in Fig. 2 for $NdBa_{2-x}La_xCu_3O_{7-\delta}$. *S* is positive in the whole temperature range and increases with increasing doping concentration. It increases with increasing temperature towards a broad maximum at T^{max} above T_c, and then decrease almost linearly up to room temperature. The plane contribution to *S* has a negative slope while the chain contribution has a positive slope [2,9,10]. These results hence indicate that the holes in the planes give the dominating contribution to the thermoelectric power.

The room temperature thermoelectric power $S_{290\,K}$ increases with increasing La content (Fig. 3), apparently associated with a decrease of hole concentration in the plane, which was estimated from the relation between the room temperature and hole concentration given by Obertelli et al. [2]. A characteristic feature of the observations is the variation of the wide peak temperature T^{max} in the $S(T)$ with doping. As can be seen in Fig. 2, T^{max} increases with increasing La doping concentration. These results for T^{max} and $S_{290\,K}$ reflect that the hole concentration

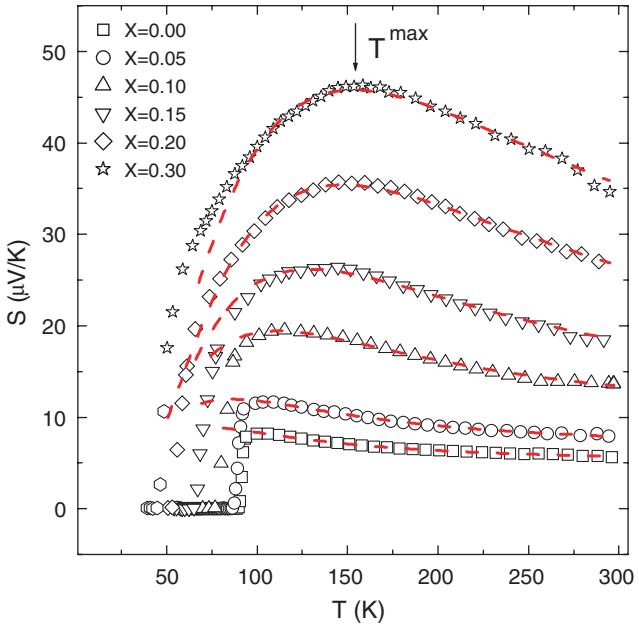

Fig. 2. Thermoelectric power S as a function of temperature and La doping for $NdBa_{2-x}La_xCu_3O_{7-\delta}$. The dashed curves are fits to the model of Eq. (1). Here T^{max} is the temperature at the maximum of $S(T)$ as shown by an arrow for one sample.

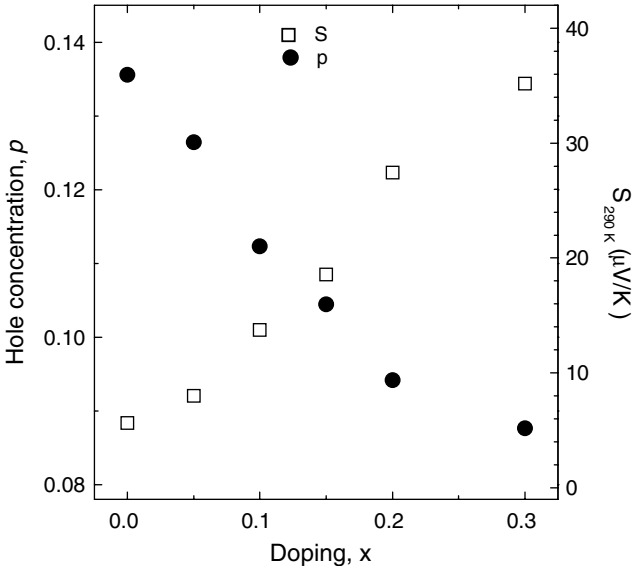

Fig. 3. Hole concentration (left hand scale), which was calculated from the universal behavior for room temperature thermoelectric power versus hole concentration of Ref. [2], and room temperature thermoelectric power (right hand scale) versus doping concentration.

decreases continuously with increasing La concentration. Published results in other high-T_c superconductors, e.g. Bi-2212 samples of varying oxygen concentration [11], and Tl-2212 doped with Y on a Ca site [12], display similar trends.

The temperature and doping concentration dependence of the resistivities $\rho(T,x)$ are shown in Fig. 4. A linear resistivity in the normal state was observed from room temperature up to T_g (dashed line in Fig. 4), where $\rho(T)$ departs from linearity, for all doped samples. The downward deviation from the T-linear behavior below T_g, which is shown by arrow in Fig. 4 for some samples, has been discussed to mark the onset of the pseudogap [13]. Increased La doping results in a change from a metal-like to a semiconductor-like behavior at low temperature and high doping concentration. The room temperature resistivity $\rho_{290\,K}$ of these samples increase linearly with increasing doping level for $x \leqslant 0.05$ and it increases faster for larger x (Fig. 5). The

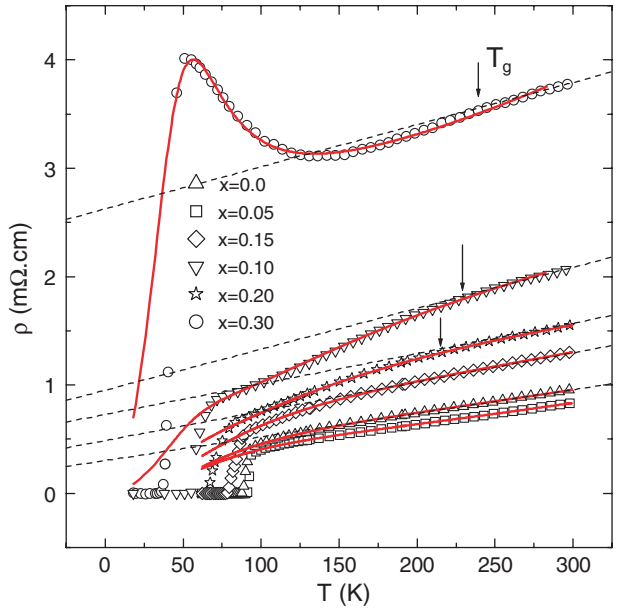

Fig. 4. The electrical resistivity ρ versus temperature T for $NdBa_{2-x}La_xCu_3O_{7-\delta}$ with $0 \leqslant x \leqslant 0.30$. The solid curves are fits to the model of Eq. (4). The dashed lines are the linearly temperature dependence of the resistivity at high temperature. Here T_g is the pseudogap temperature, which is shown the deviation of $\rho(T)$ from the T-linear behavior, as shown by an arrow for some samples.

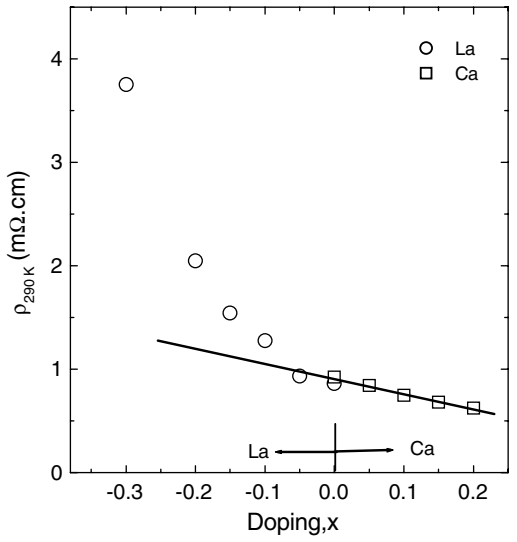

Fig. 5. The room temperature resistivity $\rho_{290\,K}$ versus La doping concentration. Data for Ca doping in Nd-123 samples have been taken from Ref. [15]. The solid line is a guide to the eye.

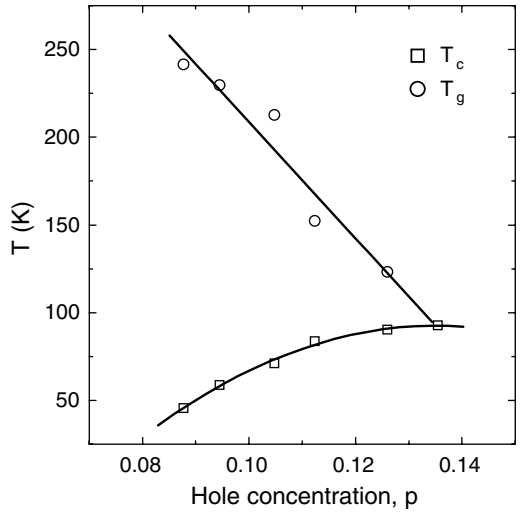

Fig. 6. Superconducting transition temperatures T_c and the pseudogap temperature T_g for La doped samples versus doping concentration. The solid curve and line is a guide to the eye.

results suggest a simple impurity effect for $x \leqslant 0.05$ and a weakening metallic state for larger x. The linear change in $\rho_{290\,K}$ at low doping level is also in agreement with observation on Ca-doped Nd-123 [15] as illustrated in Fig. 5 by similar behavior on the hole doped side. Therefore, the La doping makes the $NdBa_{2-x}La_xCu_3O_{7-\delta}$ system accessible far into the underdoped region. The strong decrease in the conductivity can be also described in the basic a schematic picture [14] for the variation of the density of states around the Fermi energy with doping concentration. With increasing La content the Fermi energy moves towards the localized part of the band at the tail of the density of states. With further doping it enters the localized part, diminishing the number of free charge carriers, and causes the conductivity decrease strongly. These results, e.g. the strong increase in the room temperature resistivity for $x \geqslant 0.05$, suggested that hole filling picture is not only mechanism to decrease hole concentration but there is also another mechanism such as mobile hole localization.

The critical temperature T_c, which is defined from the mid point of the resistive transition is shown in Fig. 3, and T_g are shown in Fig. 6 for $NdBa_{2-x}La_xCu_3O_{7-\delta}$. La doping results in a lower T_c and a larger T_g. The observed results can be explained by a decrease in the total hole concentration in the planes. Since partial substitution with La^{3+} for Ba^{2+} introduces additional electron carrier in the structure and decrease the hole concentration in the planes.

4. Semiemperical models for transport properties

The normal state transport properties were analyzed within two models. These models are the bipolaron model [6] and a phenomenological narrow band model [7].

4.1. Phenomenological narrow band model

In the phenomenological model by Gasumyants et al. [7] it is assumed that the Fermi energy is located inside a narrow energy interval within which the density of states is larger than beyond this interval. Approximate analytical expressions were derived for the temperature dependence of the transport coefficients. Results for $S(T)$ were obtained in terms of the energy bandwidth for the density of states, w_D, the band filling fraction F (i.e., the electron concentration divided by the number of states in the band), and the bandwidth w_σ of the effective conductivity $\sigma(\varepsilon)$. $\rho(T)$ and $S(T)$ can be written as

$$S = -\frac{k_B}{e} \times \left\{ \frac{w_\sigma^*}{\sinh w_\sigma^*} \left[\ln \frac{e^{\mu^*} + e^{w_\sigma^*}}{e^{\mu^*} + e^{-w_\sigma^*}} \right] - \mu^* \right\} \quad (1)$$

$$\rho = \frac{1}{\langle\sigma\rangle} \frac{1 + z^{-2} + 2z^{-1}\cosh w_\sigma^*}{z^{-1}\sinh w_\sigma^*} \quad (2)$$

$$\mu^* = \frac{\mu}{k_B T} = Ln \frac{\sinh(F w_D^*)}{\sinh[(1-F) w_D^*]} \quad (3)$$

for each sample. Here $w_D^* = w_D/(2k_BT)$, $w_\sigma^* = w_\sigma/(2k_BT)$, $z = \exp(\mu^*)$. μ is the electron chemical potential and k_B the Boltzmann constant. $\langle\sigma\rangle$ is the averages of the longitudinal conductivity in the intervals w_σ.

We have fitted our $S(T)$ data to Eq. (1) as shown by the dashed curves in Fig. 2. Results are obtained for the fraction of electron filling $F(x)$, and the two parameters $w_D(x)$ and $w_\sigma(x)$, referring to the band widths of the density of states and itinerant electrons, respectively. It was found that $F(x)$ increased by increasing x, which is suggested a decreased hole density, consistent with the expectation valence considerations. The relative concentration dependence of $F(x)$ is illustrated in Fig. 7b.

Both $w_D(x)$ and $w_\sigma(x)$ bandwidths increase strongly with x. They changed in the interval 0.14–0.7 meV and 0.05–0.11 meV, respectively, and are in agreement with results for Y-123 samples doped by oxygen reduction or addition of different 3d metals [7]. The relative increase of the both parameter are shown in Fig. 7a.

The resistivity data was also analyzed within the phenomenological narrow band model according to Eq. (2) (the curves are not shown in Fig. 4). Obtained parameters from the thermoelectric power data were used for analyzing. Typical errors are large, and they increase with increasing doping concentration. Thus the results show that the resistivity analyses are not good according to this model.

4.2. Bipolaron model

Bipolarons in oxide superconductors formed by the interaction of holes with optical phonons [16]. In the bipolaron model the normal state dynamics is dominated by

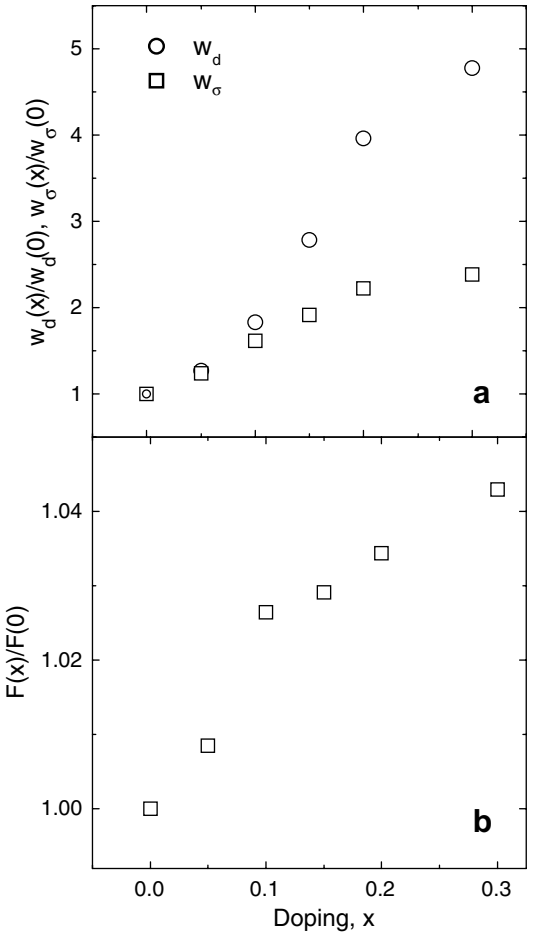

Fig. 7. Results from the phenomenological narrow band model for $NdBa_{2-x}La_xCu_3O_{7-\delta}$. The relative concentration dependence of the (a) bandwidths w_D and w_σ, (b) band filling $F(x)$.

small polarons. All the polarons (holes) are bounded into bipolarons at any temperature and the superconducting state is a charged $2e$ Bose–Einstein condensate of bipolarons. There are also thermally single polarons, which are responsible for small deviation from linearity of the normal state resistivity in underdoped cuprates at T_g temperature where a gap in the density of state appears [17]. In this model, the main point taken into consideration is the localization of the carriers by disorder [18]. This model gives the in-plane resistivity as a function of temperature [19]

$$\rho = \rho_0 \frac{(T/T_l)^2 + \exp(-\omega/T)}{\left[1 + A(T/T_c)y^{1/2}\exp(-T_g/T)\right]} \quad (4)$$

$$y \approx 1 - \exp(-T_0/T) \quad (5)$$

where $\rho_0 = bm_b/[2e^2(x - n_L)]$, x is the doping concentration, and n_L is the number of the localized carriers. $T_l = (b/a)^{1/2}$, where a is itinerant carriers scattering contribution and b is the optical phonons scattering contribution. $A = (m_b/m_p)^{5/2} \approx 6$ is the ratio of bipolaron and polaron masses. $T_0 = \pi(x - n_L)/m_b \approx T_c$, T_g is the pseoudogap temperature, and ω is optical phonons energy.

The curves in Fig. 4, which show the resistivity as a function of temperature and doping concentration $\rho(x, T)$, illustrate the fits to bipolaron model according to Eq. (4). As can be seen in Fig. 4, the model describes remarkably the experimental data particularly the nonlinear temperature dependence of the in-plane resistivity. The results for fitting parameters ρ_0, T_l, and ω are shown in Table 1. The optical phonons frequency ω and T_l increases with doping up to $x \leqslant 0.20$ as observed in the neutron scattering experiments. For $x = 0.30$, these parameters decrease because at low temperature a metal-like behavior change to a semiconductor-like. The pseudogap shows the same behavior as observed in other experiments [20].

Table 1
Doping dependence of the material parameters obtained from the fit of the resistivity experimental data to bipolaron model (Eq. (4))

x	ρ_0 (mΩ cm)	ω (K)	T_l (K)
0.00	2.97	170.36	289.76
0.05	7.04	235.98	341.86
0.10	19.48	306.93	413.42
0.15	57.39	441.95	643.90
0.20	115.13	501.29	656.53
0.30	260.64	383.15	278.97

5. Brief discussion

Two different models used to analyze transport properties of $NdBa_{2-x}La_xCu_3O_{7-\delta}$. These models are based on different assumptions and therefore are difficult to compare quantitatively. However, there is a parameter in each model that shows localization trends. This common trend in the doping dependence of such parameter gives strengthened support for the outlines of a qualitative physical picture.

In the phenomenological model, the tendency for Anderson localization at the band edges can be conveniently described by the parameter $c = w_\sigma/w_D$. The development of the energy bandwidth for the density of states w_D and the bandwidth w_σ of the effective conductivity $\sigma(\varepsilon)$ with doping reflect a change of the metallic character. The increase of w_D is stronger than the change of w_σ. Thus c decrease with increasing doping concentration, as seen in Fig. 8. This suggests an increasing tendency for localization, which mainly occurs in the localized parts of the band, and increasing electronic disorder for increased x.

In bipolaron model, the number of carrier localization $(x - n_L)$ by disorder were calculated from the parameters $\rho_0 = bm_b/[2e^2(x - n_L)]$ and $T_0 = \pi(x - n_L)/m_b \approx T_c$ obtained from the analyses of $\rho(x, T)$. The relative doping dependence of $(x - n_L)$ for $NdBa_{2-x}La_xCu_3O_{7-\delta}$ is also shown in Fig. 8 for comparison. This parameter decreases with doping concentration. It suggested an increased in the number of localization carriers by increasing doping concentration.

In summary the transport properties of polycrystalline samples of $NdBa_{2-x}La_xCu_3O_{7-\delta}$ have been studied in the normal state. Both resistivity and thermoelectric power increased with increasing La doping concentration. The resistivity results were suggested a decreased mobile hole

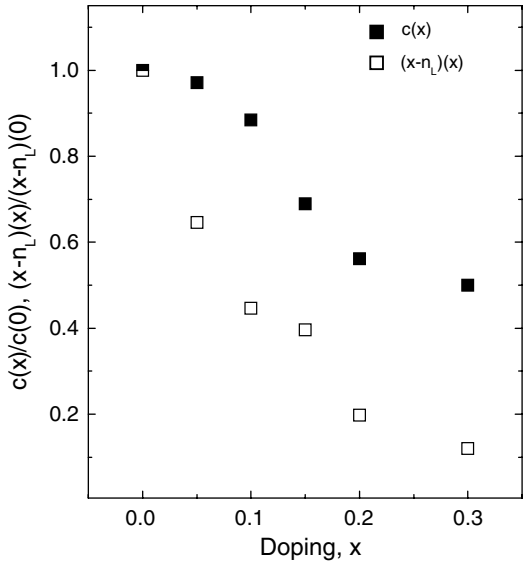

Fig. 8. Relative doping concentration dependence of the localization parameter c from the phenomenological narrow band model and $(x - n_L)$ parameter from bipolaron model.

concentration by localization mechanism in addition of hole filling. The critical temperature and pseudogap changed strongly by doping. Two different models used to analyze transport properties data. The analyses of both models give a consistent picture of La doping concentration. Both models suggested an increased tendency for hole localization and supported the resistivity results.

References

[1] B. Batlogg, H.Y. Hwang, H. Takagi, R.J. Cava, H.L. Kao, Physica C 235–240 (1994) 130.
[2] S.D. Obertelli, J.R. Cooper, J.L. Tallon, Phys. Rev. B 46 (1992) 14928.
[3] J.L. Tallon, Physica C 176 (1991) 547.
[4] J.L. Tallon, N.E. Flower, Physica C 204 (1993) 237.
[5] P.W. Anderson, Phys. Rev. Lett. 67 (1991) 2092.
[6] A.S. Alexandrov, N.F. Mott, Supercond. Sci. Technol. 6 (1993) 215.
[7] V.E. Gasumyants, V.I. Kaidanov, E.V. Valadimirskaya, Physica C 248 (1995) 255.
[8] K.E. Johansson, P.E. Werner, J. Phys. E 13 (1989) 1289.
[9] J.L. Tallon, J.R. Cooper, P.S.I.P.N. de Silva, G.V.M. Williams, J.W. Loram, Phys. Rev. Lett. 75 (1995) 4114.
[10] G.V.M. Williams, M. Staines, J.L. Tallon, R. Meinhold, Physica C 258 (1996) 273.
[11] L. Forro, J. Lukatela, B. Keszei, Solid State Commun. 73 (1990) 501.
[12] S. Keshri, J.B. Mandal, P. Mandal, A. Poddar, A.N. Das, B. Ghosh, Phys. Rev. B 47 (1993) 9048.
[13] T. Ito, K. Takenaka, S. Uchida, Phys. Rev. Lett. 70 (1993) 3995.
[14] S.R. Ghorbani, P. Lundqvist, M. Andersson, M. Valldor, Ö. Rapp, Physica C 353 (2001) 77.
[15] S.R. Ghorbani, M. Andersson, Ö. Rapp, Physica C 390 (2003) 160.
[16] A.S. Alexandrov, Phys. Rev. B 53 (1996) 2863.
[17] A.S. Alexandrov, A.M. Bratkovsky, N.F. Mott, Phys. Rev. Lett. 72 (1994) 1734.
[18] N.F. Mott, Physica C 205 (1993) 191.
[19] A.S. Alexandrov, V.N. Zavaritsky, S. Dzhumanov, Phys. Rev. B 69 (2004) 52505.
[20] D. Mihailovic, V.V. Kabanov, K. Zagar, J. Demsar, Phys. Rev. B 60 (1999) 6995.